Evidence that the tumor-suppressor protein BRCA2 does not regulate cytokinesis in human cells

Sergey Lekomtsev[1], Julien Guizetti[2], Andrei Pozniakovsky[3], Daniel W. Gerlich[2] and Mark Petronczki[1,*]

[1]Cell Division and Aneuploidy Laboratory, Cancer Research UK London Research Institute, Clare Hall Laboratories, Blanche Lane, South Mimms, Hertfordshire, EN6 3LD, UK
[2]Institute of Biochemistry, Swiss Federal Institute of Technology Zurich (ETHZ), Schafmattstrasse 18, CH-8093 Zurich, Switzerland
[3]Max Planck Institute for Molecular Cell Biology and Genetics, Pfotenhauerstrasse 108, D-01307 Dresden, Germany
*Author for correspondence (mark.petronczki@cancer.org.uk)

Summary

Germline mutations in the tumor-suppressor gene *BRCA2* predispose to breast and ovarian cancer. BRCA2 plays a well-established role in maintaining genome stability by regulating homologous recombination. BRCA2 has more recently been implicated in cytokinesis, the final step of cell division, but the molecular basis for this remains unknown. We have used time-lapse microscopy, recently developed cytokinesis assays and BAC recombineering (bacterial artificial chromosome recombinogenic engineering) to investigate the function and localization of BRCA2 during cell division. Our analysis suggests that BRCA2 does not regulate cytokinesis in human cells. Thus, cytokinesis defects are unlikely to contribute to chromosomal instability and tumorigenesis in *BRCA2*-related cancers.

Key words: BRCA2, Cytokinesis, Chromosomal instability, Cell division, Mitosis

Introduction

Heterozygous germline mutations in *BRCA2* (*Breast Cancer 2, early onset*) are associated with an increased risk of developing breast and ovarian cancer (Venkitaraman, 2002). BRCA2, a large 384 kDa protein, plays a key role in the repair of DNA damage by means of homologous recombination. It regulates the function of the Rad51 recombinase and is required for the formation of nuclear Rad51 foci (Thorslund and West, 2007). Cells that are deficient in BRCA2 are sensitive to ionizing radiation and accumulate chromosomal rearrangements (Sharan et al., 1997; Yu et al., 2000).

BRCA2-deficient cells not only show structural chromosome aberrations but also exhibit an increase in chromosome and centrosome number (Tutt et al., 1999; Yu et al., 2000). Both latter defects point towards a potential role for BRCA2 in the regulation of mitosis. Consistent with this notion, analysis of murine and human cells lacking BRCA2 function revealed defects in cytokinesis, the final stage of cell division (Daniels et al., 2004).

Cytokinesis is the process that partitions segregated sister genomes to nascent daughter cells at anaphase by virtue of ingression of a cleavage furrow (Barr and Gruneberg, 2007). The process is driven by the constriction of a membrane-coupled actomyosin ring and completed by membrane fusion (abscission) yielding two distinct daughter cells. The formation and positioning of the cleavage furrow relies on the spindle midzone, a microtubule-based structure that forms at anaphase between the segregating sister chromatids and concentrates a number of cytokinesis regulators (Barr and Gruneberg, 2007). Interestingly, BRCA2 was reported to accumulate at the spindle midzone (Daniels et al., 2004; Jonsdottir et al., 2009).
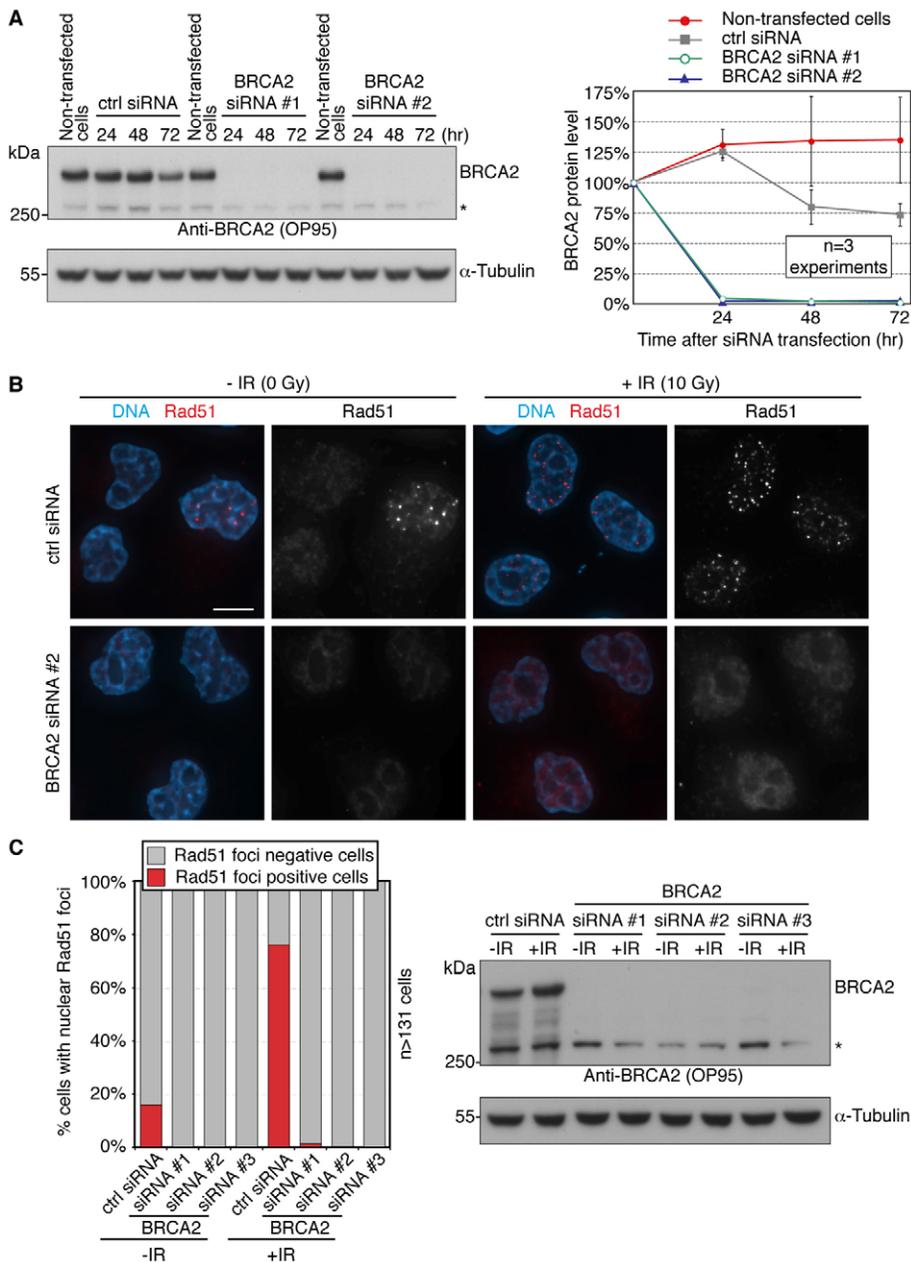
Although it is currently unknown whether defects in cell division caused by mutations in *BRCA2* contribute to tumorigenesis, a number of recent studies have suggested that tetraploidy caused by cell-division failure might be a transient intermediate on the road to aneuploidy and cancer (Ganem et al., 2007). The sociomedical importance of BRCA2 underscores the need to understand its cellular functions. At present, the molecular basis of the role of BRCA2 in cell division is unknown. It is furthermore unclear whether the cytokinetic defects observed upon loss of BRCA2 reflect the direct involvement of the protein in the process or whether they are an indirect consequence of chromosomal lesions and defective DNA repair. To address these questions, we examined the function and localization of human BRCA2 during cell division.

Results and Discussion

To investigate the consequences of acute loss of BRCA2 function, we used several small interfering RNA (siRNA) duplexes (see supplementary material Fig. S1) to deplete the protein in HeLa cells (Fig. 1). Quantitative immunoblotting revealed that, as early as 24 hours after transfection, the levels of BRCA2 protein were reduced to below 5% of the levels observed in non-transfected cells (Fig. 1A). This reduction was sufficient to abolish the formation of irradiation-induced and irradiation-independent nuclear Rad51 foci (Fig. 1B,C). Thus, our siRNA approach is capable of quantitatively depleting BRCA2 protein and blocking its well-established function in homologous recombination (Venkitaraman, 2002).

To assess the effects of BRCA2 depletion on cytokinesis, we compared HeLa cells that were transfected with siRNA duplexes targeting BRCA2 or MgcRacGAP, a component of the central spindle and essential regulator of cytokinesis (Barr and Gruneberg, 2007). Whereas depletion of MgcRacGAP resulted in the accumulation of bi-nucleated and multi-nucleated cells, a signature phenotype of defective cytokinesis, depletion of BRCA2 did not (Fig. 2A). Time-lapse analysis of cells transfected with *MgcRacGAP* siRNA revealed a failure in cleavage furrow ingression that resulted in formation of bi-nucleated cells after mitotic exit (Fig. 2B; see supplementary material Movie 1). By contrast, in cells transfected with *BRCA2* siRNA duplexes,

Fig. 1. Quantitative depletion of BRCA2 following siRNA transfection abrogates formation of nuclear Rad51 foci. (**A**) At left, immunoblot analysis of total cell lysates prepared from HeLa cells at the indicated time points after transfection with non-targeting control (ctrl) siRNA and *BRCA2* siRNAs (#1 and #2). The asterisk in this and the following figures indicates a non-specific band. At right, fluorescent immunoblotting quantification of BRCA2 protein levels after siRNA transfection relative to BRCA2 protein levels in non-transfected cells. Error bars indicate standard deviation. (**B**) Immunofluorescence images of HeLa cells transfected with control siRNA and *BRCA2* siRNA #2. Cells were exposed to ionizing radiation (IR) 48 hours after transfection. Non-irradiated (–IR) and irradiated (+IR) cells were fixed 4 hours after exposure and stained for DNA and Rad51. Scale bar: 10 µm. (**C**) At left, quantification of Rad51-positive (more than five nuclear Rad51 foci) and Rad51-negative cells (five or less foci). At right, immunoblot analysis of BRCA2 and α-tubulin protein levels 52 hours after siRNA transfection.

ingression of the cleavage furrow after anaphase onset separated nascent daughter cells (Fig. 2B; see supplementary material Movie 1). Consistent with these observations, DNA content analysis by flow cytometry showed that targeting MgcRacGAP or culturing cells in blebbistatin (Straight et al., 2003), a non-muscle myosin II inhibitor that blocks cytokinesis, led to the emergence of polyploid cells, whereas depletion of BRCA2 failed to do so (Fig. 2C). Taken together, our data strongly suggest that BRCA2 is not essential for the successful completion of cytokinesis in human cells.

Late cytokinetic defects, for example, during the process of abscission, are difficult to discern by conventional light microscopy. To scrutinize the consequences of BRCA2 depletion on these events, we used a recently developed diffusion-based assay (Steigemann and Gerlich, 2009; Steigemann et al., 2009). This approach allows us to precisely determine the time of abscission and cell separation by probing the cytoplasmic continuity of

postmitotic daughter cells. Repeated activation of photoactivatable GFP (PAGFP) in one daughter cell results in an increase of fluorescence in the non-activated daughter cell as long as the cytoplasm of the nascent cells is connected. Cessation of this increase indicates that abscission has taken place (Fig. 3A). Conditions that interfere with the completion of cytokinesis delay abscission by up to several hours when measured using this diffusion-based assay (Steigemann et al., 2009). The disassembly of microtubule bundles that are associated with the midbody normally accompanies abscission and the completion of cytokinesis. Time-lapse analysis of cells stably expressing RFP–α-tubulin and PAGFP revealed no alteration in the timing of abscission and the disassembly of midbody-associated microtubules after depletion of BRCA2 (Fig. 3B,C; see supplementary material Movie 2). These results indicate that BRCA2 does not regulate late cytokinetic events.
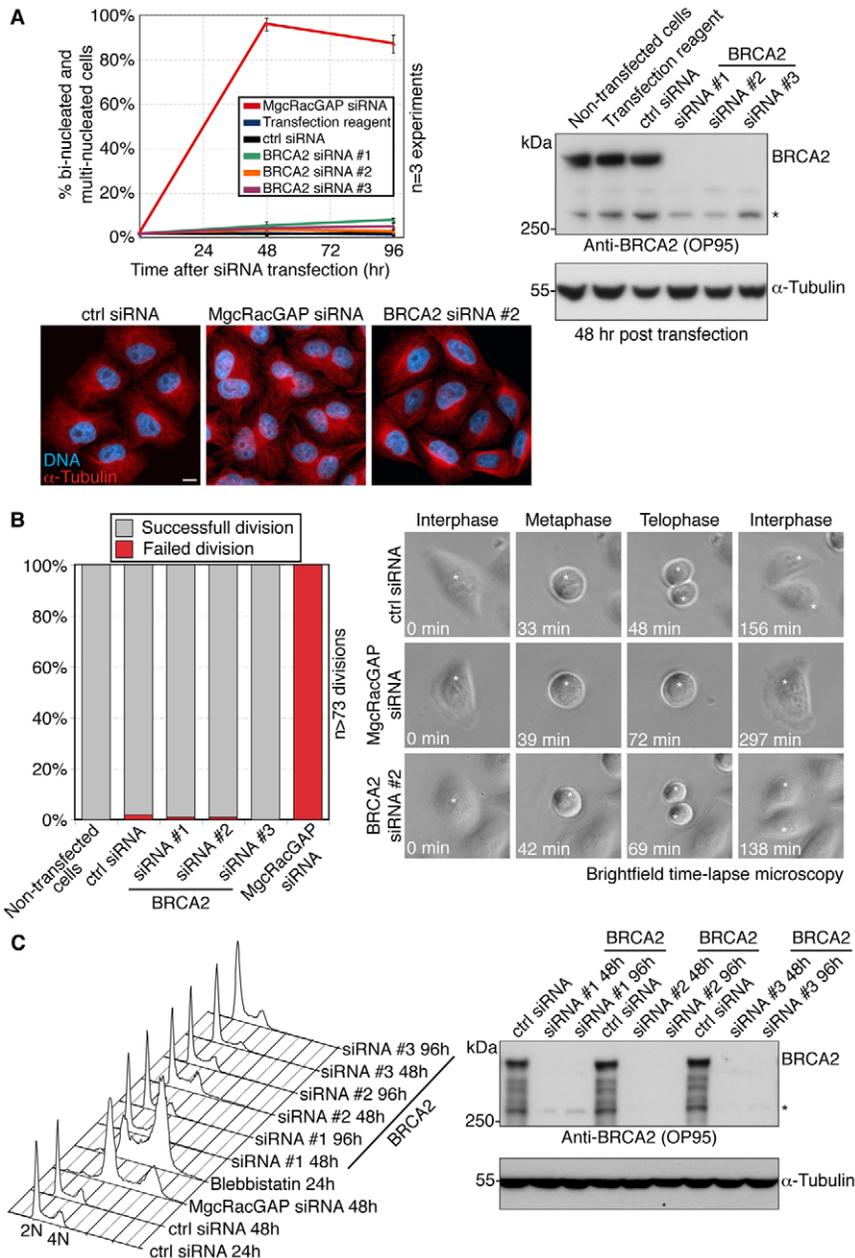
Fig. 2. Depletion of BRCA2 by siRNA does not lead to cytokinesis failure. (**A**) Quantification of bi-nucleated and multi-nucleated HeLa cells after transfection with non-targeting control (ctrl), *BRCA2* and *MgcRacGAP* siRNA duplexes or treatment with transfection reagent only. Error bars represent standard deviation. Bottom left, immunofluorescence images of HeLa cells 48 hours after transfection with the indicated siRNAs. Scale bar: 10 μm. (**B**) Quantification of successful and failed cell divisions determined using a 16 hour bright-field time-lapse recording of HeLa cells. Analysis was performed 48 hours after transfection with the indicated siRNAs. At right, selected frames from time-lapse series. Asterisks indicate individual cells. (**C**) Flow cytometry analysis of DNA content in HeLa cells at the indicated time points after transfection with siRNA duplexes or after treatment with 30 μM blebbistatin.

Residual protein persisting after depletion of BRCA2 might mask potential cytokinesis defects. To investigate the consequences of genetic inactivation of BRCA2, we used DLD1 colon cancer cell lines in which one or both alleles of *BRCA2* were disrupted by gene targeting (Fig. 4A) (Hucl et al., 2008). The modified locus encodes a truncated BRCA2 protein that lacks the C-terminal half and is slightly shorter than the protein expressed in CAPAN-1 cells, a commonly used *BRCA2* mutant cell line (Fig. 4A). Because the visual identification of two distinct postmitotic daughter cells was not possible in the DLD1 cell background, the presence of two individual mitotic cells during the second round of division was used as a surrogate indicator of a successful first division. This approach unequivocally identified cell division failure in parental *BRCA2*+/+ DLD1 cells treated with the myosin II inhibitor blebbistatin during time-lapse analysis (Fig. 4B,C; see supplementary material Movie 3). By contrast, the vast majority of

BRCA2+/+, *BRCA2*+/– and *BRCA2*–/– DLD1 cells successfully completed the first division (Fig. 4B,C; see supplementary material Movie 3). Furthermore, the small fraction of cells that have failed in cytokinesis was not increased in *BRCA2*–/– cells compared with *BRCA2*+/– DLD1 cells. Thus, targeted disruption of BRCA2 does not prevent successful cytokinesis.

BRCA2 has been reported to accumulate at the spindle midzone and midbody, consistent with its proposed role in cytokinesis (Daniels et al., 2004; Jonsdottir et al., 2009). To investigate the localization of BRCA2 during cell division, we modified a human bacterial artificial chromosome (BAC) carrying the *BRCA2* locus by inserting FLAP tags at the N terminus (NFLAP) or C terminus (CFLAP) of the *BRCA2* coding sequence using homologous recombination (Fig. 5A) (Poser et al., 2008). The selected human BAC complements BRCA2 deficiency in murine cells (Kuznetsov et al., 2008). It harbors 32 kb of upstream and 57 kb of downstream
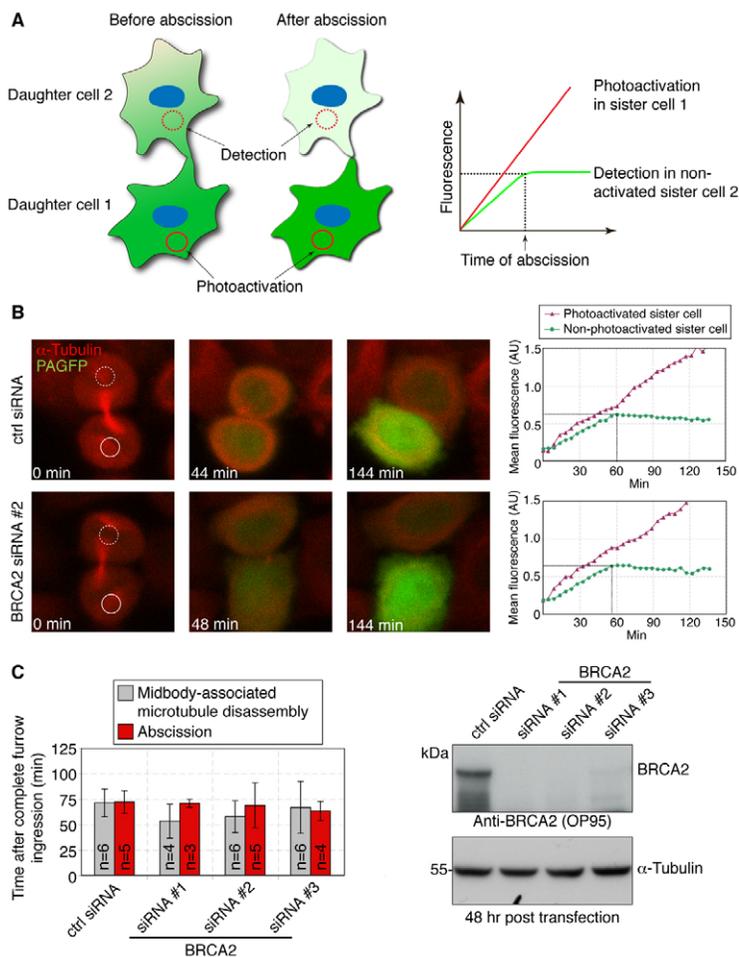
Fig. 3. BRCA2 depletion does not alter the timing of abscission or midbody-associated microtubule disassembly. (**A**) Schematic representation of the diffusion-based assay for abscission timing. (**B**) Selected frames from time-lapse series of HeLa cells stably expressing RFP-α-tubulin and PAGFP 48 hours after transfection with control or *BRCA2* siRNA duplexes. The time point t=0 minutes was set to the time of complete cleavage furrow ingression. Abscission was probed by repeated partial activation of PAGFP in one daughter cell (solid circle) and detection of PAGFP fluorescence in the non-activated daughter cells (dashed circle). At right, mean fluorescence intensity in the activated and non-activated cells is plotted in arbitrary units (AU). Abscission was determined from cessation of the increase in fluorescence in the non-activated cell (t=60 minutes for control and 54 minutes for *BRCA2* siRNA #2 in the examples shown). (**C**) Time of midbody-associated microtubule disassembly and abscission was determined by observing RFP-α-tubulin fluorescence and using the diffusion-based assay described in A.
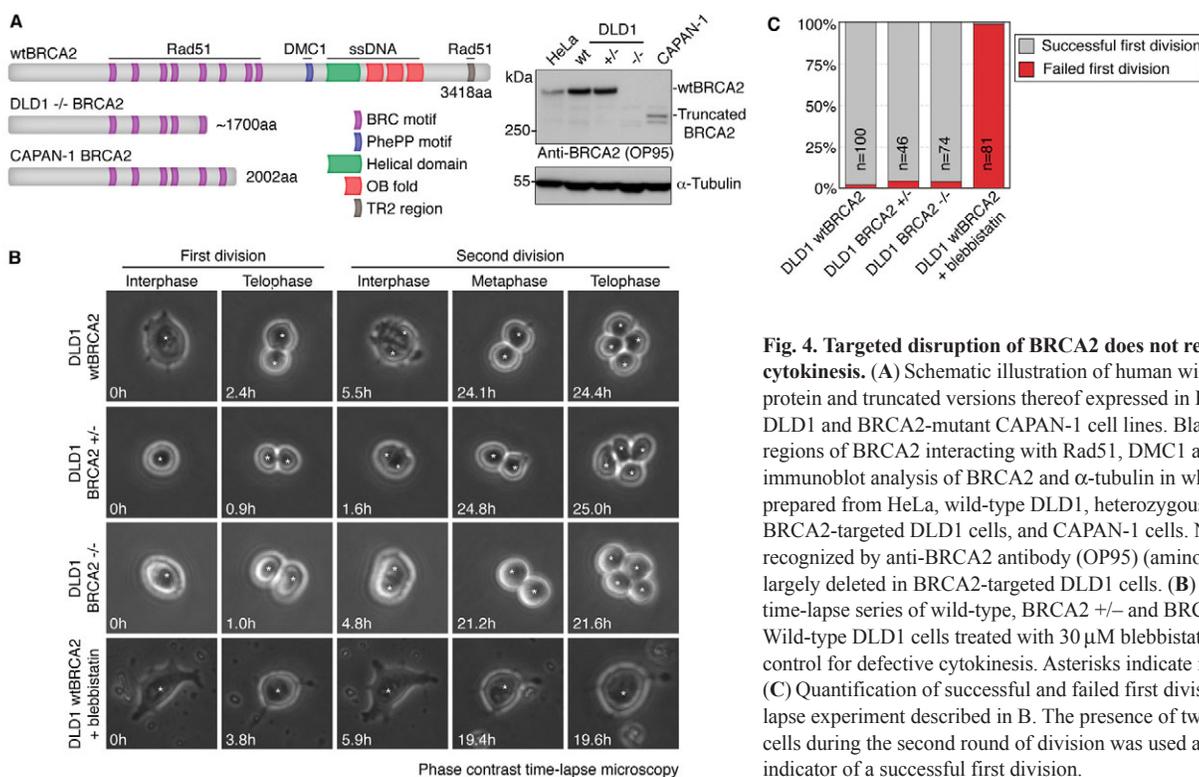
Fig. 4. Targeted disruption of BRCA2 does not result in defective cytokinesis. (**A**) Schematic illustration of human wild-type BRCA2 protein and truncated versions thereof expressed in BRCA2-targeted DLD1 and BRCA2-mutant CAPAN-1 cell lines. Black lines indicate regions of BRCA2 interacting with Rad51, DMC1 and ssDNA. At right, immunoblot analysis of BRCA2 and α-tubulin in whole cell lysates prepared from HeLa, wild-type DLD1, heterozygous and homozygous BRCA2-targeted DLD1 cells, and CAPAN-1 cells. Note that the epitope recognized by anti-BRCA2 antibody (OP95) (amino acids 1651-1821) is largely deleted in BRCA2-targeted DLD1 cells. (**B**) Selected frames from time-lapse series of wild-type, BRCA2 +/– and BRCA2 –/– DLD1 cells. Wild-type DLD1 cells treated with 30 μM blebbistatin were used as a control for defective cytokinesis. Asterisks indicate individual cells. (**C**) Quantification of successful and failed first divisions in the time-lapse experiment described in B. The presence of two individual mitotic cells during the second round of division was used as a surrogate indicator of a successful first division.
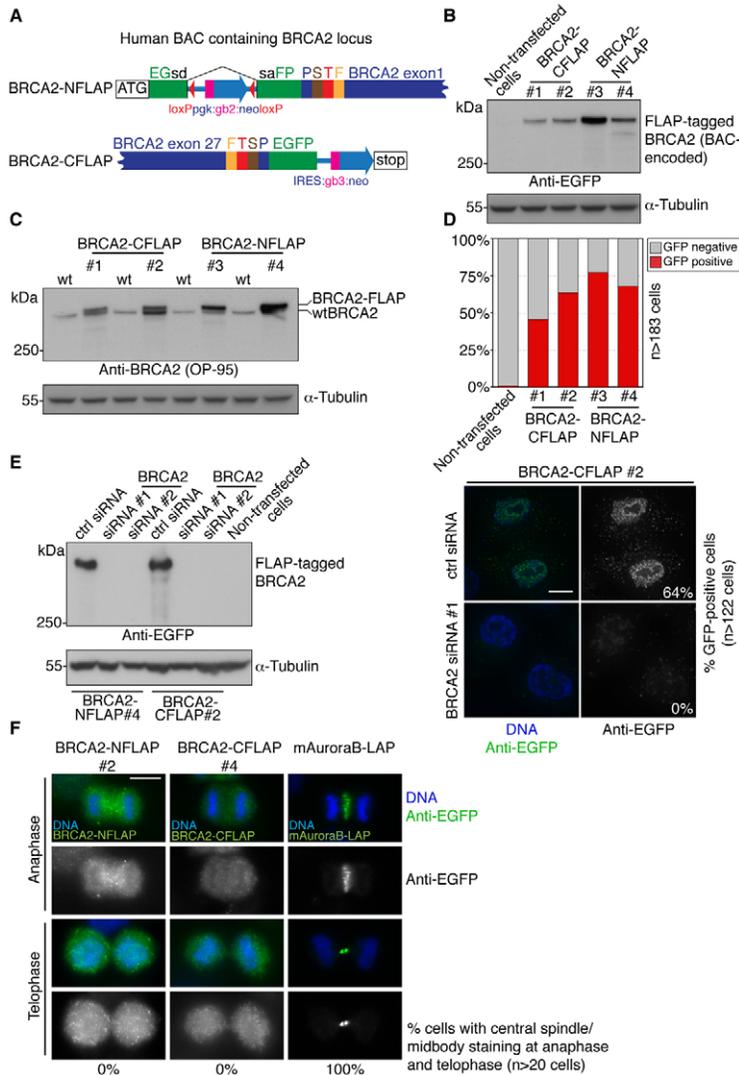
Fig. 5. BAC-encoded and epitope-tagged BRCA2 does not localize to the spindle midzone or midbody. (**A**) Schematic representation of FLAP tagging cassettes integrated at the N and C terminus of the human *BRCA2* locus encoded on BAC RP11-777I19. EGFP, enhanced green fluorescent protein; P, prescission protease cleavage site; S, S-peptide; sa, splice acceptor; sd, splice donor; T, TEV cleavage site; F, Flag. (**B**) Immunoblot analysis of FLAP-tagged BRCA2 and α-tubulin protein levels in whole cell lysates of HeLa cell lines stably expressing CFLAP- or NFLAP-tagged BRCA2. (**C**) Immunoblot analysis of endogenous and FLAP-tagged BRCA2 and α-tubulin protein levels in whole cell lysates of HeLa cell lines stably expressing CFLAP- or NFLAP-tagged BRCA2. (**D**) Quantification of EGFP-positive cells in HeLa cell lines stably expressing FLAP-tagged BRCA2. (**E**) Immunoblot analysis of FLAP-tagged BRCA2 protein levels in whole cell extracts prepared 48 hours after transfection with non-targeting control (ctrl) and *BRCA2* siRNA duplexes. At right, immunofluorescence images of HeLa cells stably expressing CFLAP-tagged BRCA2 and fixed 48 hours after transfection with control and *BRCA2* siRNA duplexes. (**F**) Immunofluorescence images of HeLa cells stably expressing FLAP-tagged BRCA2 and LAP-tagged mouse Aurora B. The structure of the LAP tag is identical to the one of the CFLAP tag shown above except that the LAP tag lacks a Flag epitope.

genomic sequence, which should facilitate the production of this unusually large protein. Stable clones expressed full-length BAC-encoded NFLAP-tagged or CFLAP-tagged BRCA2 at levels close to that of the endogenous protein (Fig. 5B,C,D). The tagged versions of BRCA2 accumulated in the nucleus of interphase cells and were efficiently depleted after transfection with *BRCA2* siRNA duplexes, confirming specificity of detection (Fig. 5E). Biochemical analyses revealed that tagged BRCA2 associates with known BRCA2-interaction partners (Tina Thorslund and Stephen West, Cancer Research UK – London Research Institute, UK, personal communication). Crucially, NFLAP- and CFLAP-tagged BRCA2 did not accumulate at the spindle midzone or midbody in anaphase and telophase cells (Fig. 5F). By contrast, BAC-encoded and LAP-tagged Aurora B kinase, a subunit of the chromosomal passenger complex and key regulator of cytokinesis, was readily detected at these structures (Fig. 5F). Re-examination of the original serum directed against BRCA2 (Daniels et al., 2004) revealed that it recognized a protein in cell extracts that migrates slightly faster than BRCA2 and that is not sensitive to BRCA2 depletion by siRNA duplexes. Although the serum labeled the spindle midzone and midbody during cytokinesis, these signals persisted after BRCA2 depletion (see supplementary material Fig. S2B), indicating

that the serum recognizes an unrelated protein. Collectively, our data suggest that BRCA2 does not localize to cytokinetic structures.

In contrast to a previous study (Daniels et al., 2004), our analysis has revealed no evidence of cytokinetic defects in human cells with compromised BRCA2 function. This suggests that BRCA2 neither directly nor indirectly regulates cytokinesis. Careful analysis of the duration of mitosis in BRCA2-depleted cells showed no delay in mitotic progression (see supplementary material Fig. S3 and supplementary material Movie 4), indicating that BRCA2 might not be involved in the control of cell division at all. Consistent with this notion, we found that BRCA2 does not localize to mitotic structures.

We employed RNA interference (RNAi) and a targeted allele to investigate the consequences of acute and constitutive loss of BRCA2 function, respectively. The experiments performed by transfection of siRNA duplexes are validated by the use of multiple duplexes targeting different regions of BRCA2, the careful quantification of the reduction in protein level following transfection and finally the inability of BRCA2-depleted cells to form Rad51 foci. The previously published report (Daniels et al., 2004) implicating BRCA2 in cytokinesis relied on the analysis of BRCA2 depletion by siRNA pools, *BRCA2*-mutant CAPAN-1 cells and

mouse embryonic fibroblasts (MEFs) carrying a truncated allele. Off-target effects of siRNA pools, genetic alterations unrelated to BRCA2 in CAPAN-1 cells, and the compromised cellular fitness of MEFs homozygous for a *BRCA2* truncation could have contributed to the detection of the reported cytokinesis defects.

Although we cannot exclude that BRCA2 is involved in the control of cell division in some cell types, our results indicate that defects in cytokinesis are unlikely to represent the primary cause of chromosomal instability and to contribute to tumorigenesis in BRCA2-deficient cancers.

Materials and Methods

Cell culture and siRNA transfection

HeLa 'Kyoto' cells and HeLa 'Kyoto' cells stably expressing RFP-α-tubulin and PAGFP were grown according to Lenart et al. (Lenart et al., 2007) and Steigemann et al. (Steigemann et al., 2009), respectively. HeLa cell lines stably expressing FLAP-targeted BRCA2 protein were grown in medium supplemented with 400 μg/ml G418 geneticin. DLD1 (Hucl et al., 2008) and CAPAN-1 (Goggins et al., 1996) cells were grown in medium supplemented with 20% FCS. For RNAi experiments, HeLa cells were transfected in suspension with 10 nM non-targeting control (Stealth RNAi negative control low GC, medium GC and high GC), 10 nM *BRCA2* siRNA duplex or 20 nM *MgcRacGAP* siRNA duplex (MgcRacGAP RACGAP1HSS120934) using Lipofectamine RNAiMAX (Invitrogen). Details of *BRCA2* siRNA duplexes are listed in supplementary material Fig. S1. Cells were grown in medium supplemented with 30 μM blebbistatin (Sigma) (Straight et al., 2003) for 24 hours (Fig. 2C) or 8 hours (Fig. 4B). For flow cytometry, cells were fixed and stained with 50 μg/ml propidium iodide (Sigma).

Western blotting

The following primary antibodies were used: mouse monoclonal anti-BRCA2 (1:100; OP95, Calbiochem), mouse monoclonal anti-EGFP (1:1000; clones 7.1 and 13.1, Roche), rabbit polyclonal anti-BRCA2 (Daniels et al., 2004) (1:500) and mouse monoclonal anti-α-tubulin (1:50,000; B512, Sigma). For protein quantification, secondary antibodies conjugated to IRDye 680 (1:5000; LI-COR) were used for detection. Protein bands were quantified using an Odyssey scanner and Odyssey v2.1 software (LI-COR). For Fig. 1A, BRCA2 protein signals were normalized to the signal intensity of α-tubulin.

Immunofluorescence microscopy

Cells were fixed with 4% formaldehyde and stained as described previously (Lenart et al., 2007). Images were acquired on a Zeiss Axio Imager M1 microscope using a Plan-Neofluar 40×/1.3 oil objective lens (Zeiss) equipped with an ORCA-ER camera (Hamamatsu) and controlled by Volocity 4.3.2 software (Improvision). Images are displayed as single *z* planes (Fig. 2A; Fig. 5F; supplementary material Fig. S2B) or maximum-intensity projections of deconvolved *z* planes (generated by the Volocity iterative restoration function) that were acquired in 0.1 μm sections (Fig. 1B; Fig. 5E). The following primary antibodies were used: mouse monoclonal anti-EGFP (1:1000; clones 7.1 and 13.1, Roche), rabbit polyclonal anti-BRCA2 (Daniels et al., 2004) (1:500), mouse monoclonal anti-α-tubulin (1:10,000; B512, Sigma) and rabbit polyclonal anti-Rad51 (1:500; FBE2) (Tarsounas et al., 2003). DAPI and secondary antibodies conjugated to Alexa-Fluor-488 or Alexa-Fluor-568 (Invitrogen) were used for detection.

Time-lapse microscopy

Before imaging, the medium was changed to phenol-red-free CO_2-independent medium (Lenart et al., 2007). Frames were acquired using a Plan-Apochromat 10×/0.45 objective on an Axio Observer Z1 microscope (Zeiss) controlled by SimplePCI software (Hamamatsu), equipped with a full-enclosure environmental chamber heated to 37°C (Digital Pixel Imaging) and an Orca 03GO1 camera (Hamamatsu). Frames were recorded every 3 minutes for a total of 16 hours (Fig. 2B; supplementary material Fig. S3A) or every 5 minutes for a total of 60 hours (Fig. 4B). The timing of abscission and midbody-associated microtubule disassembly was determined according to Steigemann et al. (Steigemann et al., 2009).

BAC recombination

Human BAC RP11-777I19 (Invitrogen) was altered by homologous recombination using the BAC modification kit (Gene Bridges) (Poser et al., 2008). CFLAP and NFLAP tagging cassettes were amplified by PCR from the plasmids R6Kamp_FLAP and R6kam_hNGFP (kindly provided by Tony Hyman, Max Planck Institute of Molecular Cell Biology and Genetics, Dresden, Germany), respectively.

Supplementary material available online at
http://jcs.biologists.org/cgi/content/full/123/9/1395/DC1

References

Barr, F. A. and Gruneberg, U. (2007). Cytokinesis: placing and making the final cut. *Cell* **131**, 847-860.

Daniels, M. J., Wang, Y., Lee, M. and Venkitaraman, A. R. (2004). Abnormal cytokinesis in cells deficient in the breast cancer susceptibility protein BRCA2. *Science* **306**, 876-879.

Ganem, N. J., Storchova, Z. and Pellman, D. (2007). Tetraploidy, aneuploidy and cancer. *Curr. Opin. Genet. Dev.* **17**, 157-162.

Goggins, M., Schutte, M., Lu, J., Moskaluk, C. A., Weinstein, C. L., Petersen, G. M., Yeo, C. J., Jackson, C. E., Lynch, H. T., Hruban, R. H. et al. (1996). Germline BRCA2 gene mutations in patients with apparently sporadic pancreatic carcinomas. *Cancer Res.* **56**, 5360-5364.

Hucl, T., Rago, C., Gallmeier, E., Brody, J. R., Gorospe, M. and Kern, S. E. (2008). A syngeneic variance library for functional annotation of human variation: application to BRCA2. *Cancer Res.* **68**, 5023-5030.

Jonsdottir, A. B., Vreeswijk, M. P., Wolterbeek, R., Devilee, P., Tanke, H. J., Eyfjord, J. E. and Szuhai, K. (2009). BRCA2 heterozygosity delays cytokinesis in primary human fibroblasts. *Cell. Oncol.* **31**, 191-201.

Kuznetsov, S. G., Liu, P. and Sharan, S. K. (2008). Mouse embryonic stem cell-based functional assay to evaluate mutations in BRCA2. *Nat. Med.* **14**, 875-881.

Lenart, P., Petronczki, M., Steegmaier, M., Di Fiore, B., Lipp, J. J., Hoffmann, M., Rettig, W. J., Kraut, N. and Peters, J. M. (2007). The small-molecule inhibitor BI 2536 reveals novel insights into mitotic roles of polo-like kinase 1. *Curr. Biol.* **17**, 304-315.

Poser, I., Sarov, M., Hutchins, J. R., Heriche, J. K., Toyoda, Y., Pozniakovsky, A., Weigl, D., Nitzsche, B., Hegemann, B., Bird, A. W. et al. (2008). BAC TransgeneOmics: a high-throughput method for exploration of protein function in mammals. *Nat. Methods* **5**, 409-415.

Sharan, S. K., Morimatsu, M., Albrecht, U., Lim, D. S., Regel, E., Dinh, C., Sands, A., Eichele, G., Hasty, P. and Bradley, A. (1997). Embryonic lethality and radiation hypersensitivity mediated by Rad51 in mice lacking Brca2. *Nature* **386**, 804-810.

Steigemann, P. and Gerlich, D. W. (2009). Cytokinetic abscission: cellular dynamics at the midbody. *Trends Cell Biol.* **19**, 606-616.

Steigemann, P., Wurzenberger, C., Schmitz, M. H., Held, M., Guizetti, J., Maar, S. and Gerlich, D. W. (2009). Aurora B-mediated abscission checkpoint protects against tetraploidization. *Cell* **136**, 473-484.

Straight, A. F., Cheung, A., Limouze, J., Chen, I., Westwood, N. J., Sellers, J. R. and Mitchison, T. J. (2003). Dissecting temporal and spatial control of cytokinesis with a myosin II Inhibitor. *Science* **299**, 1743-1747.

Tarsounas, M., Davies, D. and West, S. C. (2003). BRCA2-dependent and independent formation of RAD51 nuclear foci. *Oncogene* **22**, 1115-1123.

Thorslund, T. and West, S. C. (2007). BRCA2: a universal recombinase regulator. *Oncogene* **26**, 7720-7730.

Tutt, A., Gabriel, A., Bertwistle, D., Connor, F., Paterson, H., Peacock, J., Ross, G. and Ashworth, A. (1999). Absence of Brca2 causes genome instability by chromosome breakage and loss associated with centrosome amplification. *Curr. Biol.* **9**, 1107-1110.

Venkitaraman, A. R. (2002). Cancer susceptibility and the functions of BRCA1 and BRCA2. *Cell* **108**, 171-182.

Yu, V. P., Koehler, M., Steinlein, C., Schmid, M., Hanakahi, L. A., van Gool, A. J., West, S. C. and Venkitaraman, A. R. (2000). Gross chromosomal rearrangements and genetic exchange between nonhomologous chromosomes following BRCA2 inactivation. *Genes Dev.* **14**, 1400-1406.